The American Journal of Human Genetics, Volume *108*

Supplemental information

De novo structural mutation rates and gamete-of-origin biases revealed through genome sequencing of 2,396 families

Jonathan R. Belyeu, Harrison Brand, Harold Wang, Xuefang Zhao, Brent S. Pedersen, Julie Feusier, Meenal Gupta, Thomas J. Nicholas, Joseph Brown, Lisa Baird, Bernie Devlin, Stephan J. Sanders, Lynn B. Jorde, Michael E. Talkowski, and Aaron R. Quinlan

Supplemental Figures

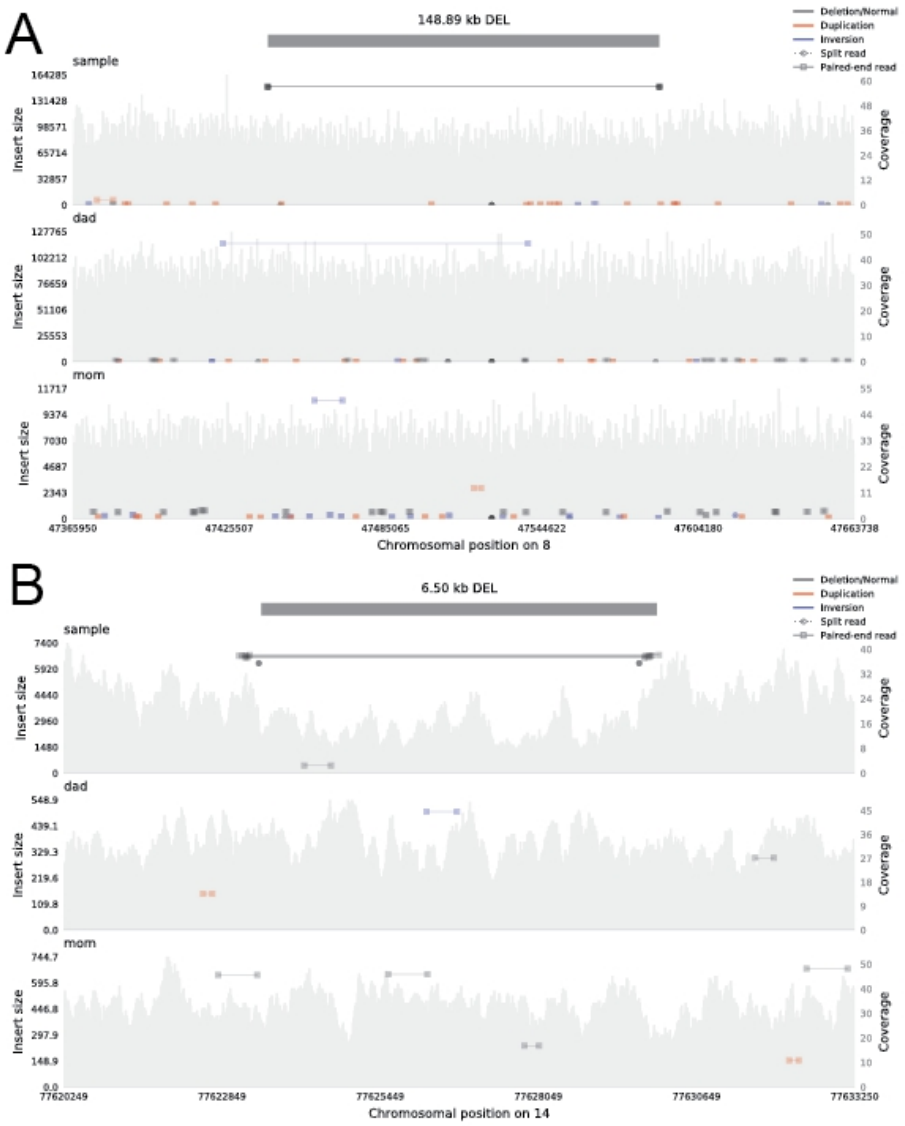

Figure S1. Somatic mosaic deletion and germline *de novo* deletion. A. A samplot image of a somatic mosaic deletion event in a sample, with both parents for contrast. Paired-end and split-read support for the variant appears, and a very slight alteration in depth-of-coverage within the deleted region. **B.** A germline *de novo* deletion in a sample, with both parents for contrast. Similar read support appears, but with a marked drop in coverage in the deleted region.

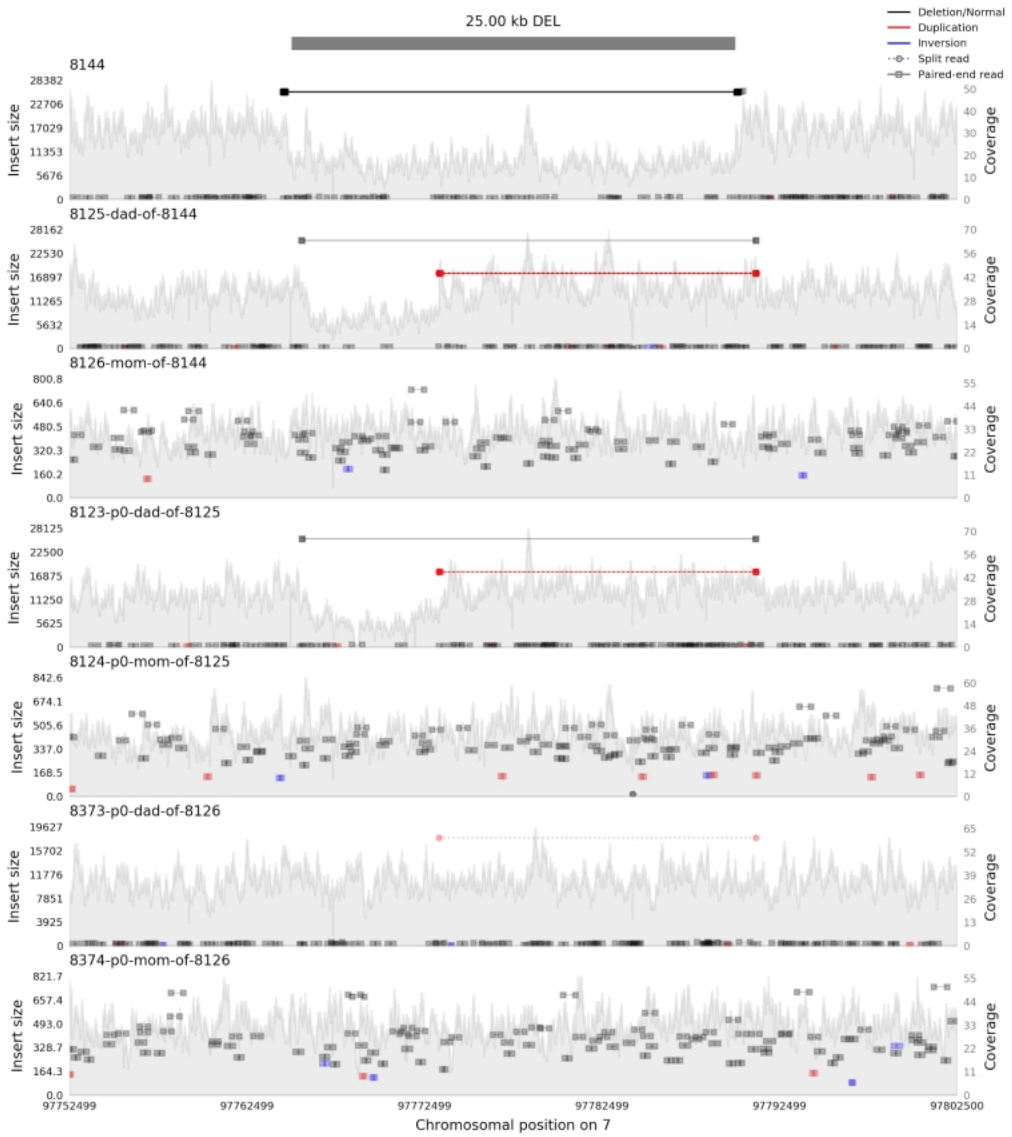

Figure S2. Sequence data for a possible false dnSV. This samplot image shows paired-end reads spanning a putative *de novo* deletion in sample 8144, with a corresponding drop in coverage. The father and paternal grandfather of 8144 have a complex variant signal in a similar region with slightly different coordinates, indicating that the deletion variant could be a partial transmission of the complex variant or an unrelated *de novo* event

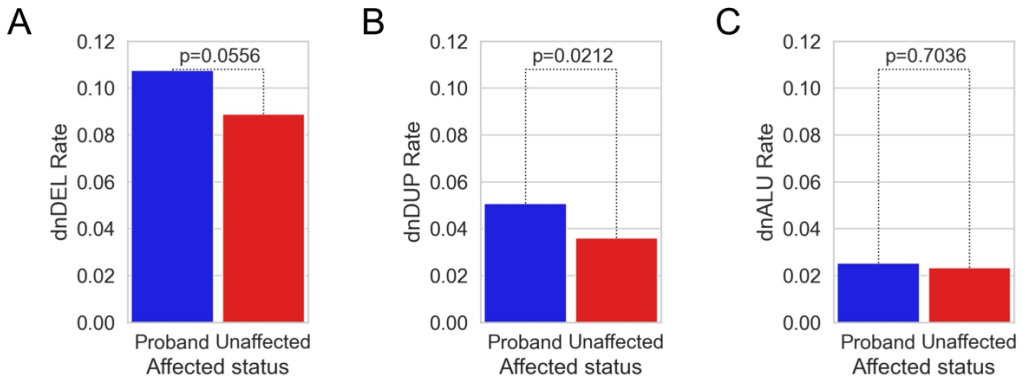

Figure S3. Comparison of rates of de novo structural variation by SV type. A. No significant enrichment for de novo deletions in probands vs. ASD unaffected samples. **B**. Significant enrichment for de novo duplications in probands vs. unaffecteds. **C**. No significant difference between *Alu* rates in probands vs. unaffecteds.

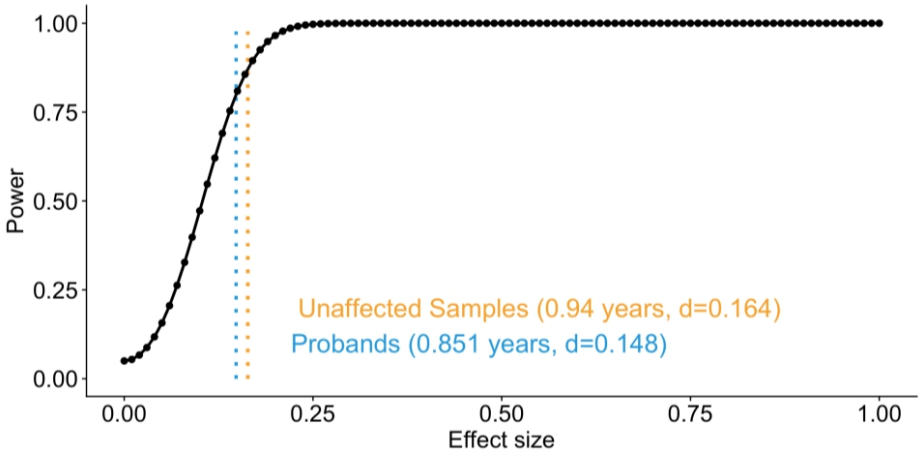

Figure S4. Analysis of power to detect a paternal age effect on dnSV rate. Cohen's d statistic was used as a measure of effect size. Dotted vertical lines indicate the minimum effect size detectable at power=0.8 for each group. The effect size, d, is given in difference in number of pooled standard deviations between means and in number of years difference in father's age between means.

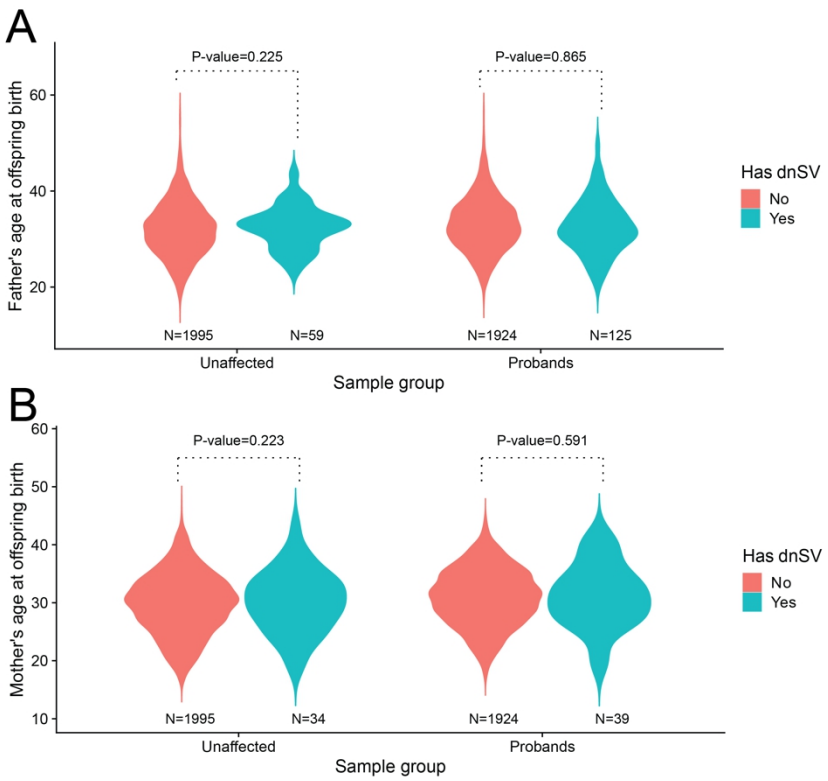

Figure S5. Correlations of parental age and de novo structural variant rate using phased variants. A. One-sided Wilcoxon rank-sum test for an increase in father's age for samples with vs without at least one paternally derived dnSV. No significant difference in either ASD unaffected samples or probands. **B.** One-sided Wilcoxon rank-sum test for an increase in mother's age for samples with vs without at least one maternally derived dnSV. No significant difference in either unaffecteds or probands.

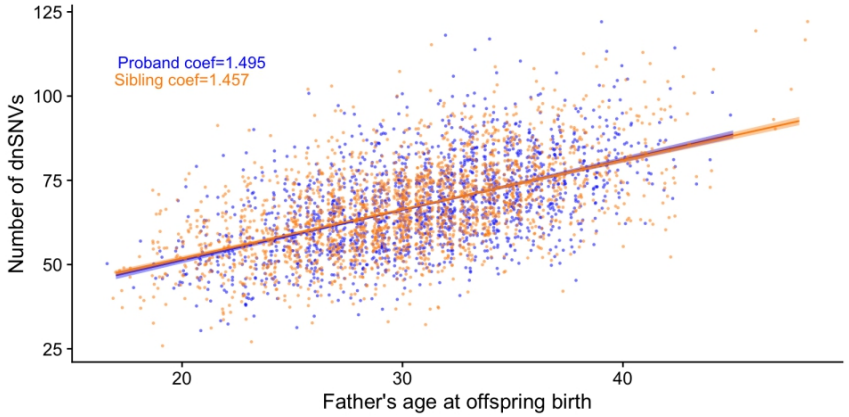

Figure S6. Correlation test between paternal age and *de novo* SNV count. A Poisson regression was used to test the correlation of the count of de novo SNVs for most samples in the CEPH and SFARI cohorts with the paternal age.

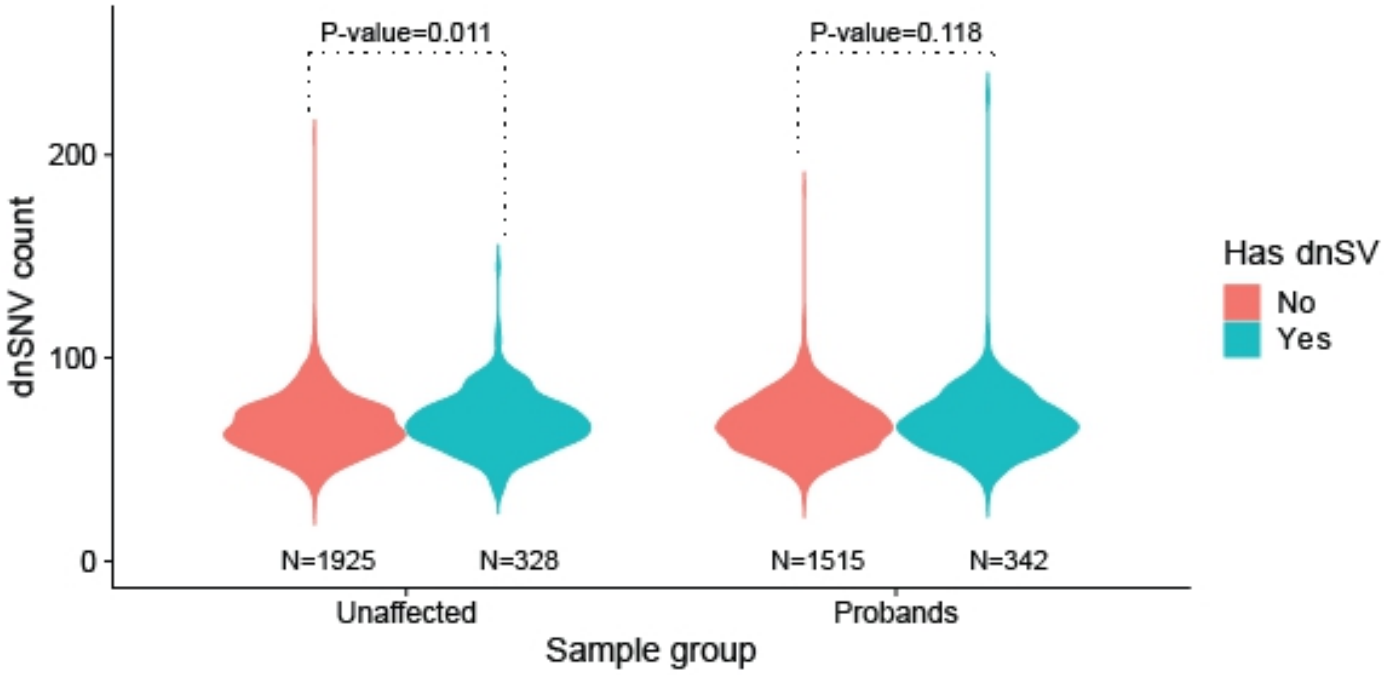

Figure S7. Correlations of *de novo* SNV count and *de novo* structural variants. One-sided Wilcoxon rank-sum test for an increase in number of dnSNVs for samples with vs. without at least one dnSV. Significant increase in dnSNV rate in when dnSV is present in ASD unaffected samples, no difference in probands.

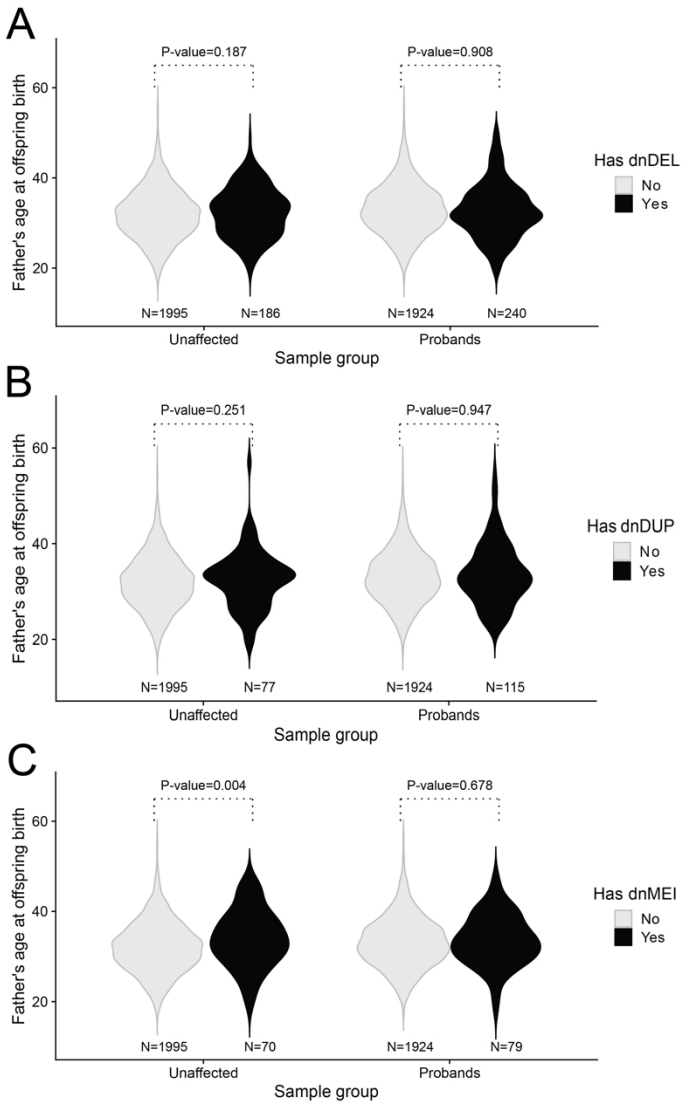

Figure S8. Correlations of paternal age and *de novo* structural variants by SV type. A. One-sided Wilcoxon rank-sum test for an increase in father's age for samples with vs. without at least one dnDEL. No significant difference in either ASD unaffected samples or probands. **B.** One-sided Wilcoxon rank-sum test for an increase in father's age for samples with vs. without at least one dnDUP. No significant difference in either unaffecteds or probands. **C.** One-sided Wilcoxon rank-sum test for an increase in father's age for samples with vs. without at least one dnDEL. Fathers of offspring with dnMEIs are significantly older among unaffecteds, but not among probands.